Proceeding of the IEEE
International Conference on Robotics and Biomimetics
Dali, China, December 2019

Design Strategy for a Surgical Manipulator based on a Compliant Mechanism
- Rigidity and Range of Motion: Finding the Optimized Balance –

Zongpeng Wu, D.S.V. Bandara, Kazuo Kiguchi, Jumpei Arata[1],
Faculty of Engineering
Kyushu University
744 Motooka, Nishi-ku, Fukuoka, 819-0395, Japan
[1]jumpei@mech.kyushu-u.ac.jp

***Abstract* - Compliant mechanisms have drawn the attention recently in developing surgical robotic manipulators for minimally invasive surgery (MIS) owing to their capabilities in making miniaturized, simple, dexterous mechanical structures. Robotically assisted MIS demands instruments with higher precision, higher output force and a higher range of motion (ROM) for better performances. On the other hand, because of the behaviour of the elastic elements, compromising these factors is challenging. In a compliant mechanism, the rigidity of the elastic element determines the precision and output force. In this paper, we study the behaviour of rigidity and the ROM of elastic elements using previously developed surgical robotic forceps based on a compliant mechanism. To tackle this problem, we studied the variation of ROM of the compliant mechanism at different rigidity values of the compliant structure by changing its thickness. The results showed the linear relationship between the ROM and the rigidity of a compliant mechanical manipulator, suggesting the optimized balance point in this trade-off.**

***Index terms* – FEA, Compliant Mechanism, Surgical Robotic Forceps, Rigidity, Range of Motion**

I. INTRODUCTION

Surgical robotic manipulators are progressively used in Minimally Invasive Surgery (MIS) where a surgeon inserts miniature instruments with multi-degree-of-freedom (DOF) into a patient body through a small incision, to perform a complex surgical task such as suturing [1]. Compared with traditional surgical procedures, MIS has significant advantages owing to smaller incisions, such as less pain, shorter hospital stay, faster recovery and lower medical costs for patients and hospital [2].

So far, number of surgical robotic manipulators with different mechanisms have been developed. Amongst, wire driven mechanisms are popular in robotic manipulators to be used in MIS. The most representative example is EndoWrist that is used in da Vinci Surgical System from Intuitive Surgical [3]. Besides, some other surgical robotic forceps based on a wire driven mechanism and using flexibly deforming tubes connected in multiple stages were presented in [4], [5] and [6], which were designed to be used in MIS. Owing to the used wire driven mechanisms, all of above studies [3] ~ [6] have advantages in miniaturized structure with multi-DOF and dexterity. However, they suffer from problems with friction and low transmission efficiency. Some other surgical robotic manipulators which use link mechanisms were presented in [7], [8] and [9]. Link mechanism has merits on rigidity but has drawbacks on miniaturization and sterilization caused by the large of number of mechanical components. In addition, two different continuum and soft robotic manipulators based on scale jamming and granular jamming for MIS are proposed in [10], [11] with the merits in flexibility and dexterity. However, they have some limitations in application because of the low rigidity and precision. To solve these problems, the surgical robotic manipulator based on compliant mechanism have drawn attention of researchers recently owing to the capabilities in making miniaturized, simple, dexterous mechanical structure.

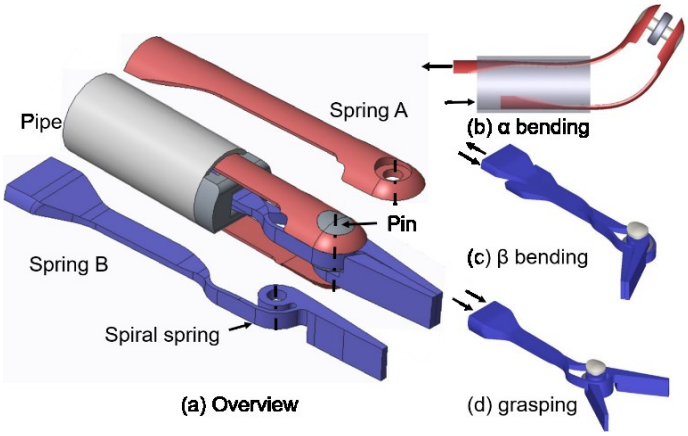

Fig. 1. Previously developed 4 DOF surgical manipulator [7]

In the authors' previous work, we proposed a surgical robotic manipulator based on a compliant mechanism which consists of largely deformable elements [12] and [13]. The overview of the developed forceps is illustrated in figure 1. Figure 1(a) illustrates the structure of the mechanism which is made of two different types of springs (Spring A and Spring B), a pipe, a spring guide and a pin joint. A pair of spring As and a pair of spring Bs are connected by a pin joint at the tip. As shown in the figure 1(b) and (c), when the distal end of one spring As or one spring Bs is pulled and the remaining spring is pushed, the forceps will bend in corresponding directions α and β respectively (α denotes motion of spring A, β denotes motion of spring B). The tip of the forceps will perform grasping when distal ends of both spring Bs are pulled or pushed together

978-1-7281-6321-5/19//$31.00 ©2019 IEEE

(illustrated in figure 1(d)). As the fourth DOF, rotational motion along the long axis is performed by rotating the pipe together with the whole structure. Thus, the manipulator has four DOF at the tip.

Benefited from the largely deformable elastic elements, the proposed manipulator has advantages in making a simple, further downsizable structure with manufacturing simplicity. However, at the same time, having elastic elements brings a trade-off between the ROM and the rigidity to the structure. In theory, a higher rigidity contributes to a higher motion accuracy and a higher output force. A larger ROM is generally preferable for a surgical manipulator. Therefore, the larger ROM and higher rigidity is suggested for better performances of a surgical manipulator. However, during the design process in the previous study, we observed a negative correlation between the ROM and the rigidity of the compliant mechanism used in the robotic forceps [12], [13]. Therefore, it is necessary for optimization of the design to identify the relationship between the ROM and the rigidity. Hence, in this study, we conducted a series of FEA simulations on the previously proposed manipulator to find out the optimized balance in design strategy. In the next section the methodology of design optimization will be introduced. It will be followed by the results of the study and discussion and conclusion.

II. Method

According to [12] and [13], spring B was revealed to have a higher strain value during the bending and grasping motions compared to that of spring A. Furthermore, spiral spring of spring B, has the thinnest dimensions compared to other dimensions of this compliant structure. Thus, two spring Bs have a high impact on the rigidity of the forceps in contributing to high output force and grasping force. Therefore, increasing the rigidity of spring B, will contribute to the higher rigidity of the whole manipulator and output force significantly. Therefore, in this study, we focus on spring B to find out the relationship between the rigidity and the ROM and identify the optimized balance in design strategy.

In order to investigate the aforementioned relationships using spring B, thickness of the spring was used as the control parameter [12], [14], [15]. Accordingly, the thickness of the spring was changed to change the rigidity of the structure. For each different thickness of the spring, two sets of FEA simulations were carried out to investigate the quantitative value of the rigidity and the ROM. The thickness of spiral spring of spring B was changed between 0.18 mm to 0.32 mm with 0.02 mm interval in between, resulting in a total 8 different simulation models. The thickness of the spring was changed by adding more material inwards to spring B. Adding more material to outer body of the spring is constrained owing to the limitation of keeping the outer diameter at 3 mm (see figure 2) and the available material size for fabrication.

FEAs were performed using a mechanism analysis software (DAFUL 2019 R1, Virtual Motion Inc., Korea) together with preprocessing software (FEMAP v11.2.2, Siemens Inc., Germany) for mesh modeling. During the simulation, the parameters of the material of spring were set to be similar to that of Ni-Ti (Young's modulus: 5,000 kgf/mm^2, Poisson ration: 0.3, yield strength ~ 237 MPa). In this study, a linear behavior of Ni-Ti material is assumed. The simulation model was meshed by tetrahedral mesh, and the mesh size was set as 0.1 mm for spiral spring and 0.25 mm for other part of spring B as shown in figure 3. The pipe, the pin and the spring guide were not considered for simulation as the main interest of the simulation lies only on spring B.

A. Finite Element Analysis for Rigidity Estimation

Figure 4 (a) shows simulation setup for the rigidity test. As shown, distal end of spring B is fixed and a 0.1N of force is applied to the tip of the spring. The tip of the forceps is expected to move down from the original position and this displacement is used to calculate the rigidity of the forceps. Then the rigidity is calculated according the equation (1), where d denotes the displacement of tip and F denotes the force applied on the tip.

$$\text{Rigidity [N/mm]} = F \,/\, d \tag{1}$$

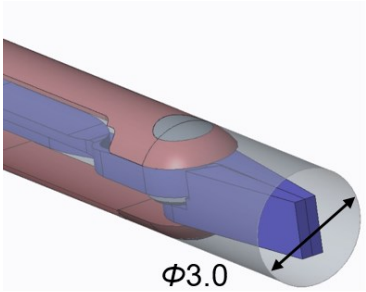

Fig. 2. Limitation of forceps from application

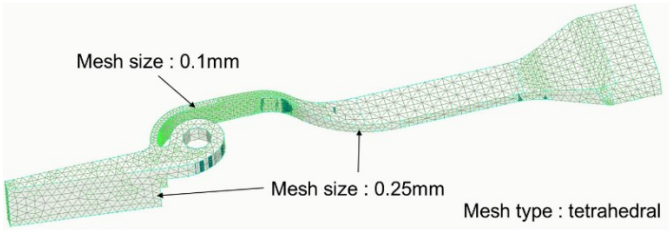

Fig. 3. Mesh setting in simulation

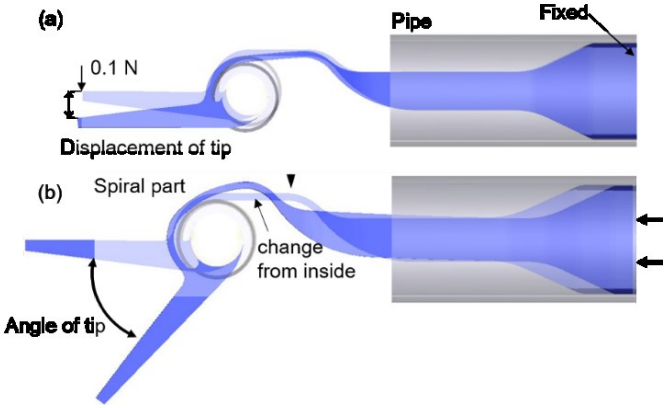

Fig. 4. (a) simulation method for Rigidity test
(b) simulation method for ROM test

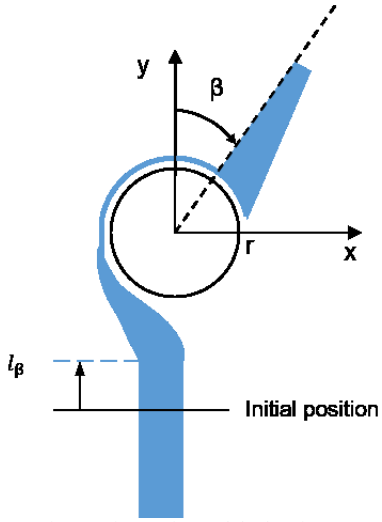

Fig. 5. Kinematic model of spring B

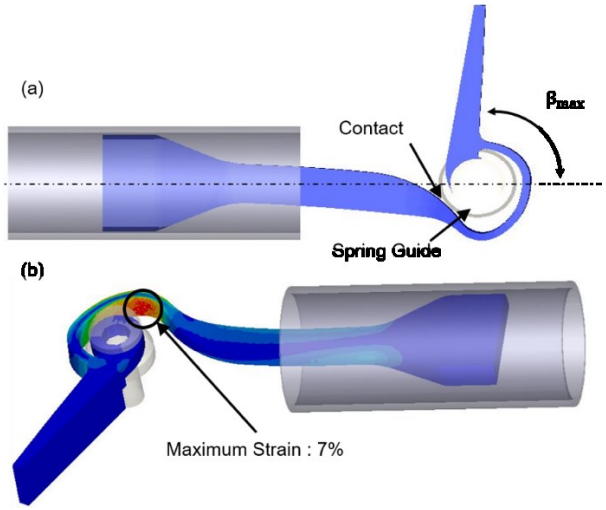

Fig. 6. Geometric constraint (a) and Material constraint (b) in the ROM estimation

B. *Finite element analysis for ROM estimation*

Figure 4 (b) shows the simulation setup for ROM test. During the simulation, the distal end of the spring B is pushed similar to the actuation method of the forceps. An overview of the kinematic model for the motion of spring B is shown in figure 5. A linear displacement input of l_β is given from the distal end of spring B. This linear motion will be translated to a rotational motion at the tip, generating an angle β. The relationship of the displacement l_β and the angle β can be shown as follows.

$$l_\beta = r\beta \tag{2}$$

During the ROM estimation using the simulation results, two different conditions are considered.

- Geometrical constraint: as shown in figure 6. (a), the streamlined connection will meet the spring guide at the maximum ROM, β_{max}.
- Material constraint: The maximum recovery strain of Ni-Ti is 7%. Maximum strain during the deformation of spring B is limited to the 7% at the maximum ROM, β_{max} (see figure 6. (b)).

From the above two conditions, when one condition is met at a certain angle, β it is considered the ROM, β_{max} of the structure.

III. Results

This section presents the results of the FEA of Rigidity estimation and the ROM estimation. At the end of the section, both two results are combined to study the relationship between the rigidity and the ROM.

A. *Rigidity Estimation*

The results of FEA for rigidity estimation are shown in Table 1 and figure. 7. FEA results show a decrement in the displacement of the tip of the forceps, when the thickness of the structure is increased (see orange line of figure 7). Thus, the rigidity of the structure can be computed using the equation (1). The variation of rigidity with the thickness of the structure is demonstrated by the blue line of figure 7. Both the displacement of tip and the rigidity of the structure change almost linearly with the change of the thickness of material according to the results. Table 1 shows the numerical values of displacement and the rigidity for different thickness of the structure.

B. *ROM Estimation*

The results of ROM test simulation are shown in Table 2. It shows the variation of ROM and the maximum strain value for different thicknesses of spring B. According to the results, the ROM during the first four set of values of thicknesses from 0.18 mm to 0.24 mm is determined by the geometrical constrain of the structure. Thus, it can reach a maximum of 88 deg of β angle. After 0.24 mm of thickness the ROM of the structure is determined by allowing the maximum deformation of the structure to be within its recovery strain of 7 %. Accordingly, increasing the thickness of the structure caused more concentration in the structure and the ROM was decreased with the increment of the thickness. The results show the ROM of the structure is decreased from 88 deg to 65 deg, when the thickness is increased from 0.24 mm to 0.32 mm.

C. *Relationship of ROM and Rigidity*

Figure 8 illustrates the combination of the above two results of ROM estimation and rigidity estimation. It shows the relationships between the rigidity, ROM and the maximum strain value. According to the results, until around 0.2 N/mm of rigidity, the structure can reach its maximum ROM, constrained by the geometrical constrain. However, when the rigidity is increased beyond 0.2 N/mm the ROM of the structure decreases linearly and ROM is determined by the material constrain by reaching its maximum recovery strain of 7%. When the rigidity of the spring is below 0.2 N/mm the maximum strain during the deformation to its ROM, decreased linearly with the rigidity.

TABLE 1

RESULTS OF RIGIDITY ESTIMATION

Thickness / [mm]	Displacement / [mm]	Rigidity / [N/mm]
0.18	1.12	0.089
0.20	0.86	0.116
0.22	0.67	0.149
0.24	0.54	0.185
0.26	0.44	0.227
0.28	0.37	0.270
0.30	0.32	0.313
0.32	0.29	0.345

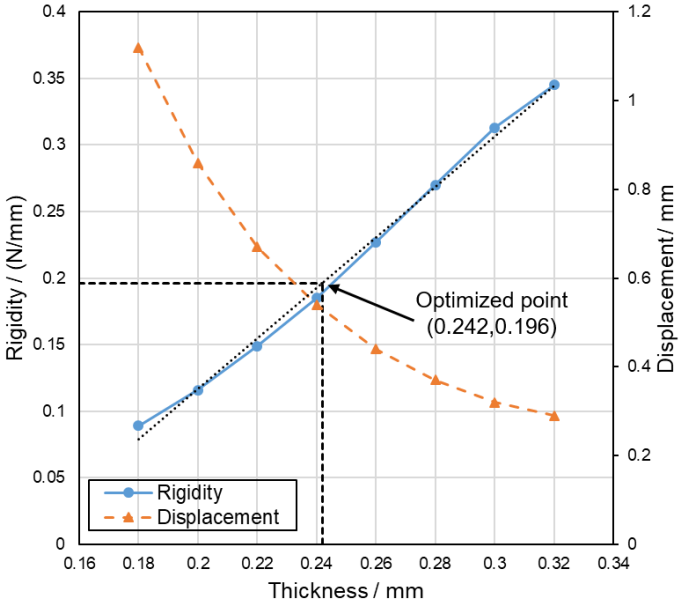

Fig. 7. Relationship between rigidity and thickness

TABLE 2

RESULTS OF ROM ESTIMATION

Thickness / [mm]	ROM / [deg]	Max strain value / %
0.18	88	4.51
0.20	88	5.36
0.22	88	6.11
0.24	88	6.84
0.26	80	7
0.28	74	7
0.30	70	7
0.32	65	7

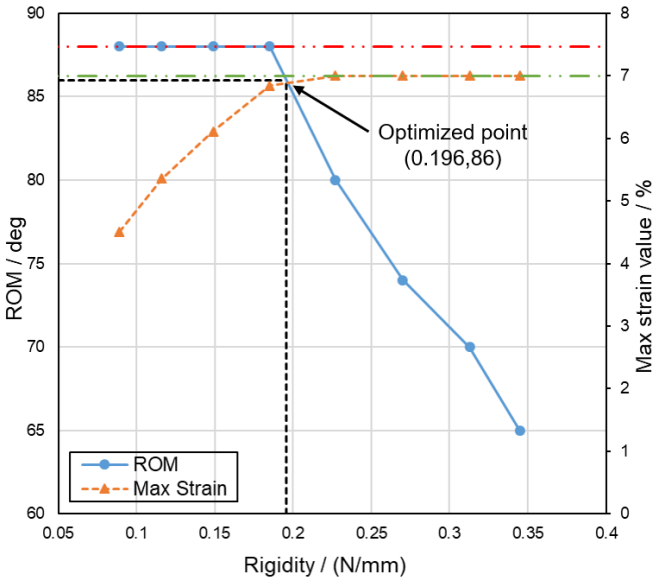

Fig. 8. Relationship between rigidity and thickness

More importantly, in this study, optimized balance point between the ROM and rigidity is determined to have a higher output force, accuracy and ROM. Thus, the optimized point can be determined from figure 8 to be at 0.19 N/mm of the rigidity. At this value the structure will have a ROM of 86 deg. The maximum strain during the deformation for ROM will be 6.9%. In the same manner, the thickness of the structure at the optimized point can be determined using graph at figure 7. From the graph the optimized thickness of the structure will be 0.242 mm.

IV. DISCUSSION AND CONCLUSION

This paper presented a study on the behaviour of the relationship of the rigidity and the ROM of elastic elements. The study was carried out using an available design of a surgical manipulator based on a compliant mechanism made of Ni-Ti. The study aimed to determine the optimized balance point of the rigidity and ROM of the structure of the compliant mechanism.

The output force and the precision of a compliant mechanism changes depending on the rigidity of the elastic element. Higher degree of rigidity of the elastic structure results in a higher output force and a higher precision and vice versa. In designing a surgical manipulator, the best combination of the output force, precision and the range of motion needs to be selected for better performances during the applications.

During the study, the rigidity of the elastic element was changed by changing the thickness of the material. The ROM and the rigidity of the elastic structure was obtained using two different finite element studies. The results of the FEA demonstrated higher thickness of the material resulted in higher rigidity of the elastic element. In a similar way higher thickness of the material caused higher strain of the material. ROM of the elastic structure was decreased with the increment of the thickness of the material. However, the range of motion of the

structure was upper bounded by the geometrical constrain at 88 deg of maximum angle. With the increment of the thickness, after 0.24 mm of thickness the range of motion was decided considering the maximum allowable strain limit of the material 7%.

Accordingly, it can be concluded when a higher ROM is expected for a target application there will be a trade-off with the lower values of output force and the precision. On the other hand, when a higher precision and output force is expected for the target application there will be a trade-off with a lower ROM of the structure. For mechanism with similar type of compliant mechanisms similar kind of behaviour can be expected between the ROM and rigidity.

In addition, with respect to the studied complaint structure, the optimized point of rigidity and ROM was found to be at 0.242 mm of thickness of the structure. This resulted in a 0.19 N/mm rigidity of the structure and a ROM of 86 deg resulting 6.9 % strain during the maximum deformation. However, it should be noted that the optimized point is defined only considering the theoretical aspects. During the practical applications the maximum strain during the maximum deformation need to be kept well below its maximum strain. ROM, rigidity and the material thickness need to be determined based on these aspects during the design process. Thus, these observations are expected to be used in a future design process of a compliant mechanism to select a better point of rigidity and ROM based on demand of the application. On the other hand, in a different study, the springs are mathematically modelled and their behaviour is studied theoretically.

ACKNOWLEDGEMENT

This work was supported by JSPS KAKENHI Grant Number JP18H03549.

REFERENCES

[1] V. Vitiello, K.-W. Kwok, G.-Z. Yang, “Introduction to robot- assisted minimally invasive surgery (MIS),” in *Medical Robotics: Minimally Invasive Surgery*, I. P. Gomes, Ed. Elsevier, 2012, pp. 1-40.

[2] P.P. Pott, H.P. Scharf, M.L.R. Schwarz, “Today’s state of the art in surgical robotics,” Computer Aided Surgery, vol.10-2, pp.101-132, 2005.

[3] Intuitive Surgical, da Vinci. [Online]. Available: https://www.intuitive.com. [Accessed Sept, 2019]

[4] N. Simaan, R. Taylor, P. Flint, “A Dexterous System for Laryngeal Surgery,” *The 2014 IEEE Conference on Robotics and Automation, ICRA 2014*, Hong Kong, China, 2014. pp.351-357.

[5] R. J. Webster, B.A. Jones, “Design and Kinematic Modeling of Constant Curvature Continuum Robots: A Review,” The International Journal of Robotics Research, vol. 29, no. 13, pp. 1661–1683, 2010.

[6] Z. Li, L. Wu, H. Ren, H. Yu, “Kinematic comparison of surgical tendon-driven manipulators and concentric tube manipulators,” Mechanism and Machine Theory, Vol. 107, pp. 148-165, 2017.

[7] H. Yamashita, D. Kim, N. Hata, T. Dohi, “Multi-Slider Linkage Mechanism for Endoscopic Forceps Manipulator,” *Proc. of IEEE/RSJ Int. Conf. Intelligent Robots and Systems*, 2003, pp.2577-2582.

[8] C. Ishii and K. Kobayashi, "Development of a New Robotic Forceps Manipulator for Minimally Invasive Surgery and Its Control," *2006 SICE-ICASE International Joint Conference*, Busan, 2006, pp. 250-253.

[9] K. Ibrahim, A. Ramadan, M. Fanni, Y. Kobayashi, A. Abo-Ismail, M. G. Fujie, “Development of a new 4-DOF endoscopic parallel manipulator based on screw theory for laparoscopic surgery,” *Mechatronics*, Vol. 28, pp. 4-17, 2015.

[10] T. Ranzani, M. Cianchetti, G. Gerboni, I. D. Falco, A. Menciassi, "A Soft Modular Manipulator for Minimally Invasive Surgery: Design and Characterization of a Single Module," *IEEE Transactions on Robotics*, vol. 32, no. 1, pp. 187-200, Feb. 2016.

[11] S. M. Hadi Sadati, Y. Noh, S. Elnaz Naghibi, A. Kaspar, T. Nanayakkara, “Stiffness Control of Soft Robotic Manipulator for Minimally Invasive Surgery (MIS) Using Scale Jamming,” in *Intelligent Robotics and Applications, ICIRA 2015*, H. Liu, N. Kubota, X. Zhu, R. Dillmann, D. Zhou, Eds. Berlin: Springer, 2015, vol.9246.

[12] J. Arata, Y. Fujisawa, R. Nakadate, K. Kiguchi, K. Harada, M. Mitsuishi, M. Hashizume, The“Compliant four degree-of-freedom manipulator with locally deformable elastic elements for minimally invasive surgery,” *Proc. Int. Conf. Robotics and Automation,* 2019, pp.2663-2669.

[13] W. Kajihara, R. Nakedate, K. Kiguchi, K. Harada, M. Mitsuishi, M, Hashizume, J. Arata, “Mechanism study on a miniaturized compliant manipulator for Minimally Invasive Surgery,” *The 14th Asian Conference on Computer Aided Surgery*, Shanghai, China, 2018.

[14] L. L. Howell. *Compliant mechanisms*. John Wiley & Sons, 2001.

[15] R. Trochimczuk, A. Łukaszewicz, T. Mikołajczyk, F. Aggogeri, A. Borboni, “Finite element method stiffness analysis of a novel telemanipulator for minimally invasive surgery,” *SIMULATION*, vol. 95, no. 11, pp. 1015–1025, 2019.